Journal of Interfaces, Thin films, and Low dimensional systems 7 (2) Winter and Spring (2024) 773-788

A review of roughness coupling effects on the contact area, interfacial separation, adhesion, and friction between an elastic solid and a hard substrate with randomly rough, self-affine fractal surfaces

Review article

Mohadeseh Feshanjerdi*, Amir Ali Masoudi*

Department of Condensed Matter Physics, Faculty of Physics, Alzahra University, Tehran, Iran

ARTICLE INFO

Article history:
Received 8 December 2023
Revised 29 December 2023
Accepted 31 January 2024
Available online 23 March 2024

Keywords
Self-affine fractal
Auto-spectral density function
Cross-correlation
Adhesive contact
Friction

ABSTRACT

When two solids are squeezed together, they generally do not make atomic contact everywhere within the nominal contact area. This fact should be considered in many technological applications due to its enormous practical implications. In this paper, we briefly review Persson's contact mechanics and then review an extended version of Persson's contact mechanics. In the extended version, we take in to account two solid surfaces which are rough before calculating the effects of surface roughness's of two solids on the area of real contact, adhesion, friction, and interfacial separation. We show that these values strongly depend on the roughness of two solids and the cross-correlation between them. Therefore, we present that there is no general mapping between systems of both surfaces being rough and self-similar, and those with only one surface being rough and self-similar.

1 Introduction

All surfaces occurring in nature and industry are rough, provided they are observed with sufficiently high magnifications (small length scales) [1-8]. So, for two contacting solid surfaces, microscopically there are many non-contact regions (the interfacial separation), and microscopic contact occurs only at a fraction of the macroscopic contact. This fraction of real contact, as well as the interfacial separation, are affected by the roughness of the surfaces and play important roles in the mechanical properties of the system. The area of real contact characterizes the frictional properties of the contact, as well as the strength of adhesion and the amount of wear [3-5]. Some other phenomena are affected by the interfacial separation: heat transfer, contact resistivity, lubrication, and sealing [5-8].

The first study on the contact mechanics of two elastic bodies has been presented by Hertz [9], where, the roughness had been introduced by a set of asperities with equally high and identical radii of curvature. Greenwood and Williamson [10] have studied the effect of roughness on the contact between a surface and a rough surface. They have assumed that roughness has asperities with spherical summits of identical radius with a Gaussian distribution of heights. In reality, however, most of the surfaces are rough on many different length scales. In the contact mechanics theory of Persson, the limitations of the above models have been addressed. In that theory, solids have randomly rough, self-affine fractal surfaces on many length scales [11-26] and the probability distribution of the contact pressure is shown to be governed by a diffusive process in terms of the magnification at the interface. In all of these works, the area of real contact between a smooth elastic solid surface and a hard substrate with randomly rough surface have been studied. However, there are essentially no surfaces which are smooth on atomic scales. Therefore, the elastic solid should be assumed to

*Corresponding author.
Email addresses: M.feshanjerdi@Alzahra.ac.ir, Masoudi@Alzahra.ac.ir
DOI: 10.22051/jitl.2024.45817.1102

have a rough surface as well. The effect of roughness of the elastic solid on the area of real contact, adhesion, friction, and the interfacial separation is studied in Refs. [27-29] by an extended version of Persson's model of contact mechanics.

In studying the contact of elastic solids with rough surfaces, the contact stresses would depend on the shape of the gap between the surfaces before loading. That is, if the height fluctuations of the surfaces are h_1 and h_2, it is (h_2 - h_1) that matters. It could seem then, that one could keep one of the surfaces (say the soft one) smooth, and consider only the other surface rough, with a fluctuation height equal to (h_2 - h_1) [1, 2, 5, 12, 13]. The point is that normally h_1 and h_2 are described each by a single set of three parameters: the Hurst exponent, the correlation length, and the root-mean-square roughness (assuming the surfaces to be self-similar). The two sets corresponding to the two surfaces are in general different from each other. Hence the relative roughness (h_2 - h_1) is normally not like the roughness of a single self-similar surface: it has two kinds of Hurst exponents, correlation lengths, and root mean-square roughness, not characteristic of a single surface [27-29]. So, the two-rough surface system is equivalent to a single-rough-surface, only if one of the rough surfaces in the latter system is not restricted to a self-similar surface.

This paper is organized as follows: Section 2 is a review of Persson's contact theory between a smooth elastic surface and a hard rough surface. In section 3, an extended version of this model is used to calculate the adhesive contact, non-adhesive contact, interfacial separation, and hysteretic friction when both contacting surfaces are randomly rough. Section 4 presents the numerical results for the extended version and compares the differences between Persson's contact theory and the extended version. Section 5 is devoted to the concluding remarks.

2 Persson's contact theory between a smooth elastic surface and a hard rough surface

In this section the main equations of Persson's contact mechanics theory are reviewed. In this theory, the interfacial is studied at different magnifications $\zeta = (L/\lambda)$ where L is the linear size of the system and λ is the length scale. The wave numbers are defined as $q = (2\pi/\lambda)$ and $q_L = (2\pi/L)$ so that $\zeta = (q/q_L)$. Persson focuses on the probability distribution $P(\sigma, \zeta)$ of the normal stress at the interface under the magnification ζ. For full contact the stress probability distribution $P(\sigma, \zeta)$ satisfies the differential equation [13]:

$$\frac{\partial P}{\partial \zeta} = f(\zeta)\frac{\partial^2 P}{\partial \sigma^2}, \tag{1}$$

where σ is the interfacial stress in the apparent contact area at the magnification ζ. f is the diffusivity function:

$$f(\zeta) = \frac{1}{2}\frac{<(\Delta\sigma_z)^2>}{\Delta\zeta} = \frac{\pi}{4}E^{*2}q_L\, q^3 \;\; C(q), \tag{2}$$

$$E^* = \frac{E}{(1-\nu^2)}, \tag{3}$$

where <...> stands for the ensemble average, and E^* is the effective elastic modulus. E and ν are the elastic modulus and the Poisson ratio, respectively. C is the Fourier transform of the correlation of heights at different locations:

$$C(\boldsymbol{q}) = \frac{1}{(2\pi)^2}\int d^2x < h(\boldsymbol{x})h(\boldsymbol{0}) > e^{-i\,\boldsymbol{q}.\boldsymbol{x}}, \tag{4}$$

where h(**x**) is the rough substrate height distribution, **x** = (x, y) is the in-plane position vector. It is assumed that Eq. (1) and Eq. (2) are correct for partial contact, and to account for partial contact the following initial and boundary conditions are introduced.

$$P(\sigma, 1) = \delta(\sigma - \sigma_0),$$

$$P(-\sigma_a, \zeta) = 0,$$

$$P(\infty, \zeta) = 0, \tag{5}$$

where $\sigma_a > 0$ is the largest tensile stress possible. The detachment stress $\sigma_a(\zeta)$ depends on the magnification and can be related to the effective interfacial energy (per unit area) $\gamma_{\text{eff}}(\zeta)$ [14, 25, 26]:

$$\sigma_a(\zeta) \approx \left[\frac{\gamma_{eff}(\zeta)Eq}{1-\nu^2}\right]^{1/2}, \tag{6}$$

$$-\gamma_{eff}(\zeta)\,A(\zeta) = U_{ad}(\zeta) + U_{el}(\zeta). \quad (7)$$

A(ζ) is the apparent contact area at the magnification ζ. The relative contact area (at the magnification ζ is given by [14]

$$\frac{A(\zeta)}{A_0} = P(\zeta),$$

$$P(\zeta) = 1 - \int_1^{\zeta} d\zeta'\, S(\zeta'), \quad (8)$$

where $S(\zeta)$ is obtained from the integral equation:

$$\exp\left\{-\frac{[\sigma_a(\zeta)+\sigma_0]^2}{4a(\zeta)}\right\} = \int_1^{\zeta} d\zeta'\, S(\zeta')\left[\frac{a(\zeta)}{a(\zeta)-a(\zeta')}\right]^{1/2} \times \exp\left\{-\frac{[\sigma_a(\zeta)-\sigma_a(\zeta')]^2}{4[a(\zeta)-a(\zeta')]}\right\},$$

$$a(\zeta) = \int_1^{\zeta} d\zeta'\, f(\zeta'). \quad (9)$$

This is numerically solved for $S(\zeta)$. $U_{el}(\zeta)$ is the elastic energy stored at the interface due to the elastic deformation of the solids at length scales shorter than λ = (L/ζ). From [16, 18]:

$$U_{el}(\zeta) \approx \frac{\pi}{2} A_0 E^* \alpha \int_{q_L}^{q_a} dq\, q^2 C(q) P(q), \quad (10)$$

where q_L and q_a are the smallest and the largest surface roughness wave numbers, corresponding to L (the size of the system) and a (the lattice spacing of the blocks), respectively. Under the nominal stress σ_a, the surface asperities do not, in general, fully penetrate inside the elastic block where the contact between the substrate and the elastic block is not full. Hence the auto-spectral density function does not contribute in full to the elastic energy stored at the interface. This aspect is taken into account in Eq. (10) through the factor αP(q). α is less than one (but of the order one), when the squeezing pressures are small this factor takes into account the fact that the elastic energy stored in the contact region is less than the average elastic energy for full contact [30]. For full contact $P(q) = 1$ (A = A0), and α = 1. The adhesion energy $U_{el}(\zeta)$ is assumed to be proportional to the apparent contact area and is calculated as [14]:

$$U_{ad}(\zeta) = -\Delta\gamma\, A(\zeta_{max}) \int_0^{\infty} dx\, (1 + \xi^2 x)^{\frac{1}{2}} e^{-x}, \quad (11)$$

$$\xi^2 = \int d^2 q\, q^2\, C(q). \quad (12)$$

The effective interfacial energy $\gamma_{\text{eff}}(\zeta)$ for partial contact is given as

$$\frac{\gamma_{\text{eff}}(\zeta)}{\Delta\gamma} = \frac{P(q_a)}{P(q_L)} \int_0^{\infty} dx\, (1+\xi^2 x)^{1/2} e^{-x} - \frac{2\pi}{\delta}\alpha \int_{q_L}^{q_a} dq\, q^2 C(q), \quad (13)$$

$$\delta = \frac{4(1-\nu^2)\Delta\gamma}{E}, \quad (14)$$

where δ is the adhesion length.

2.2 Contact area, and interfacial surface separation for a non-adhesive contact

For a non-adhesive contact, the boundary condition of the probability distribution P(σ, ζ) for the normal stress σ at the interface under the magnification ζ in Eq. (5) is [13]:

$$P(\sigma = 0, \zeta) = 0, \quad (15)$$

and for the resulting probability distribution [18, 30]

$$P(\sigma,\zeta) = \frac{1}{2(\pi G)^{1/2}}\left\{\exp\left[-\frac{(\sigma-p)^2}{4G}\right] - \exp\left[-\frac{(\sigma+p)^2}{4G}\right]\right\}, \quad (16)$$

where p is the nominal squeezing pressure and

$$G(q) = \frac{\pi}{4}\left(\frac{E}{1-\nu^2}\right)^2 \int_{q_L}^{q_a} dq\, q^3 C(q). \quad (17)$$

C(q) is the auto-spectral density function [31] of the hard randomly rough substrate. Denoting the actual (microscopic) and the nominal (macroscopic) contact areas by A and A_0, respectively, the relative contact area is:

$$\frac{A}{A_0} = \int_{0^+}^{\infty} d\sigma\, P(\sigma,\zeta) =: P(q). \tag{18}$$

So,

$$\frac{A}{A_0} = \frac{1}{(\pi G)^{\frac{1}{2}}} \int_0^p d\sigma \exp\left(-\frac{\sigma^2}{4G}\right), \\ = \operatorname{erf}\left(\frac{p}{2G^{\frac{1}{2}}}\right). \tag{19}$$

The error function can be approximated by a linear function of its argument, for the casethe argument is small. The result is

$$\frac{A}{A_0} \approx \frac{p}{(\pi G)^{1/2}}, \quad p \ll G^{1/2}. \tag{20}$$

Regarding the interfacial surface separation, let's consider an elastic block squeezed against a flat hard surface. The separation between the average surface plane of the block and the average surface plane of the substrate is denoted by $\bar{u}$, which is nonnegative. Due to the external pressure p required to produce this separation, an elastic energy is storedin the block. Denoting this by U_{el} (equation (10)), one arrives at

$$U_{el}(\bar{u}) = \int_{\bar{u}}^{\infty} du\, A_0 P(u),$$
$$p = -\frac{1}{A_0}\frac{dU_{el}}{du}. \tag{21}$$

In cases the applied normal squeezing pressure p is small, the surface asperities do notfully penetrate into the elastic block and only a partial contact is realized and $P(q)$ in (10) is given by [1, 13]:

$$P(q) = \frac{1}{\sqrt{\pi}} \int_0^{S(q)p} dx \exp(-x^2). \tag{22}$$

$$S(q) = \frac{w(q)}{E^*}. \tag{23}$$

$$w(q) = \left[\pi \int_{q_L}^{q} dq\, q^3\, C(q)\right]^{-1/2}. \tag{24}$$

Substituting Eqs. (3), (10), (24), and (23) in (21), after calculations it is shown thatfor non-adhesive interactions and small applied pressures, the relation between the average interfacial separation $\bar{u}$ and the small applied normal squeezing pressure p is [30, 32].

$$p \approx \beta E^* \exp\left(-\frac{\bar{u}}{u_0}\right),$$
$$\bar{u} \approx u_0 \log\left(\frac{\beta E^*}{p}\right), \tag{25}$$

where

$$u_0 = \sqrt{\pi}\,\alpha \int_{q_L}^{q_a} dq\, q^2 C(q)\, w(q), \tag{26}$$

$$\beta = \varepsilon \exp\left\{-\frac{\int_{q_L}^{q_a} dq\, q^2 C(q) w(q) \log[w(q)]}{\int_{q_L}^{q_a} dq\, q^2 C(q) w(q)}\right\}, \tag{27}$$

$$\varepsilon = \exp\left[\int_0^{\infty} dx\, 2x \log x \exp(-x^2)\right] \approx 0.7493. \tag{28}$$

3.2 Hysteretic contribution of smooth rubber friction on therough concrete surface

The hysteretic friction model developed by Persson [1] is based on the energy dissipation ΔE. As the rubber slides on a hard rough surface, oscillatory forces are experienced by it, which cause energy being dissipated in the rubber. This corresponds to the nominal frictional stress σ_f experienced by rubber. The calculation is based on an integral of contributions due to different wavelengths (wave numbers). In [1], equations have been derived which describe the friction on a rubber block which is pressed on a rough surface. The frictional stress σ_f is equal to $\mu\sigma_0$, where σ_0 is the normal stress. One has

$$\mu \approx \frac{1}{2} \int_{q_0}^{q_a} dq\, q^3 C(q)\, P(q) \\ \int_0^{2\pi} d\phi \cos\phi\, \operatorname{Im}\left[\frac{E(-qu\cos\phi)}{\sigma_0(1-\nu^2)}\right]. \tag{29}$$

where E is the complex viscoelastic modulus of the rubber block and $C(q)$ is the auto- spectral density function of the hard randomly rough surface.

Experiments have shown that a typical road surface [24] and a polished surface by an abrasive paper (polished styrene butadiene rubber (SB)) [39] can be approximated by self-affine fractals. The frequency is written in terms of the slip velocity

$$\frac{u}{\lambda} = \boldsymbol{q}.\boldsymbol{u} = qu, \tag{30}$$

where ϕ is the angle between the sliding direction and the wave vector $\boldsymbol{q}$. ν, the Poisson's ratio of the rubber block, is assumed to be independent of frequency and equal to 0.5. The integration in Eq. (29) is performed over the wave vectors. The normalized contact area $P(q)$ is defined as:

$$P(q) = \frac{A}{A_0}$$
$$= \frac{2}{\pi}\int_0^{\infty} dx\, \frac{\sin x}{x} \exp[-x^2 G(q)]$$
$$= erf\left[\frac{1}{2\sqrt{G(q)}}\right], \tag{31}$$

$$G(q)$$
$$= \frac{1}{8}\int_{q_0}^{q_a} dq\, q^3 C(q) \int_0^{2\pi} d\phi\, \mathrm{Im}\left|\frac{E(-qu\cos\phi)}{\sigma_0(1-\nu^2)}\right|^2. \tag{32}$$

3 Two randomly rough surfaces in contact with each other

3.1 Effective interfacial energy for an adhesive contact

The elastic energy stored in the vicinity of the asperity contact regions due to a flat elasticsurface being in contact with the rough surface of a hard substrate is [17]:

$$U_{el} \approx -\frac{1}{2}\int d^2x\, \langle u_z(\boldsymbol{x})\sigma_z(\boldsymbol{x})\rangle,$$

$$= -\frac{(2\pi)^2}{2}\int d^2q\, \langle u_z(\boldsymbol{q})\sigma_z(\boldsymbol{q})\rangle, \tag{33}$$

where $u_z(\boldsymbol{x})$ and $\sigma_z(\boldsymbol{x})$ are the normal displacement field of the surface of the elastic solid and the normal stress, respectively, and $u_z(\boldsymbol{q})$ and $\sigma_z(\boldsymbol{q})$ are their Fourier transform. The relation between the normal stress and the normal displacement field of the surface of the elastic solid is [17]:

$$u_z(\boldsymbol{q}) = M_{zz}(\boldsymbol{q})\,\sigma_z(\boldsymbol{q}), \tag{34}$$

$$M_{zz}(\boldsymbol{q}) = -\frac{2(1-\nu^2)}{Eq}. \tag{35}$$

Now consider a randomly rough self-affine fractal elastic surface in contact with the randomly rough self-affine surface of a hard substrate. Equation (34) still holds but now, if full contact between the surfaces is achieved, the normal displacement field of the elastic solid is equal to the difference of the heights of the surfaces:

$$u_z(\boldsymbol{q}) = h_2(\boldsymbol{q}) - h_1(\boldsymbol{q}), \tag{36}$$

so that

$$h_2(\boldsymbol{q}) - h_1(\boldsymbol{q}) = M_{zz}(\boldsymbol{q})\,\sigma_z(\boldsymbol{q}). \tag{37}$$

Substituting Eqs. (37) and (35) in Eq. (33) results in

$$U_{el}(\zeta)$$
$$\approx \frac{(2\pi)^3 E}{4(1-\nu^2)}\int dq\, q^2\, [\langle h_2(\boldsymbol{q})\, h_2(-\boldsymbol{q})\rangle$$
$$+ \langle h_1(\boldsymbol{q})\, h_1(-\boldsymbol{q})\rangle - \langle h_1(\boldsymbol{q})\, h_2(-\boldsymbol{q})\rangle$$
$$- \langle h_2(\boldsymbol{q})\, h_1(-\boldsymbol{q})\rangle]. \tag{38}$$

the spectral density function [33] is

$$C_{ij}(\boldsymbol{q}) = \frac{(2\pi)^2}{A_0}\langle h_i(\boldsymbol{q})\, h_j(-\boldsymbol{q})\rangle, \tag{39}$$

where A_0 denotes the macroscopic (nominal) contact area (L is the diameter of the macroscopic contact area, so that $A_0 = L^2$), and i and j could be 1, 2 [34, 35]. Here the joint distribution function of the height fluctuations is assumed to be Gaussian while the surfaces are assumed to be homogeneous and isotropic. One has

$$\langle h_i(\boldsymbol{q})\, h_j(-\boldsymbol{q})\rangle = \langle |h_i(\boldsymbol{q})|^2\rangle = \frac{A_0 C_i(q)}{(2\pi)^2}, \tag{40}$$

where C_i is a real function which depends on only $q = |\boldsymbol{q}|$. One also has

$$\langle h_1(\boldsymbol{q})\, h_2(-\boldsymbol{q})\rangle = \eta_{12}(\boldsymbol{q})\sqrt{\langle|h_1(\boldsymbol{q})|^2\rangle\langle|h_2(\boldsymbol{q})|^2\rangle}\ , \quad (41)$$

where $\eta_{12}(\boldsymbol{q})$ is called the coherence function and is a complex function, the values of which are inside the unit disk in the complex plane [36, 37]. If the surfaces are homogeneous and isotropic, η_{12} would be real and depend on only q and would be equal to η_{21}. In that case the subscripts are dropped and η_{12} and η_{21} are denoted by η. Special cases are $\eta = 0$ (uncorrelated surfaces), $\eta = +1$ (completely positive correlated surfaces), or $\eta = -1$ (completely negative correlated surfaces). Here the simple case is studied that η is a constant (does not depend on $\boldsymbol{q}$). Substituting Eqs. (40) and (41) in Eq. (38) with constant η results in [27-29]:

$$U_{el}(\zeta) \approx \frac{\pi E A_0}{2(1-\nu^2)}\int dq\, q^2\ [C_1(q) + C_2(q)] - \frac{\pi E A_0}{(1-\nu^2)}\,\eta\int dq\, q^2\ \sqrt{C_1(q)C_2(q)}. \quad (42)$$

As stated earlier, the adhesion energy U_{ad} (ζ) is assumed to be proportional to the apparentcontact area. When the elastic solid has a randomly rough surface, the apparent contact area changes so that the adhesion energy changes as well. Regarding $f(\zeta)$ in Eqs. (1) and (2), it is calculated assuming full contact between the elastic solid and the hard rough substrate, as in [38]. A similar approach is followed here to calculate f (ζ) for two rough solids. Finally, one has for the stress distribution at the magnification ζ,

$$\sigma_z(\boldsymbol{x},\zeta) = \int_{|\boldsymbol{q}|<\zeta q_L} d^2q\ \sigma_z(\boldsymbol{q})\ e^{i\boldsymbol{q}.\boldsymbol{x}}. \quad (43)$$

Substituting Eq. (37) in Eq. (43) we have

$$\sigma_z(\boldsymbol{x},\zeta) = \int_{|\boldsymbol{q}|<\zeta q_L} d^2q\ M_{zz}^{-1}(\boldsymbol{q})\ [h_2(\boldsymbol{q}) - h_1(\boldsymbol{q})]\ e^{i\boldsymbol{q}.\boldsymbol{x}}. \quad (44)$$

So,

$$\Delta\sigma_z(\boldsymbol{x},\zeta) = \int_D d^2q\ M_{zz}^{-1}(\boldsymbol{q})\ [h_2(\boldsymbol{q}) - h_1(\boldsymbol{q})]\ e^{i\boldsymbol{q}.\boldsymbol{x}}, \quad (45)$$

where

$$D = \{\boldsymbol{q}|\ \zeta q_L < |\boldsymbol{q}| < (\zeta + \Delta\zeta)q_L\}. \quad (46)$$

One then arrives at

$$\langle(\Delta\sigma_z)^2\rangle = \int_D d^2q \int_D d^2q'\, M_{zz}^{-1}(\boldsymbol{q})\, M_{zz}^{-1}(\boldsymbol{q}')e^{i(\boldsymbol{q}+\boldsymbol{q}').\boldsymbol{x}} \times \langle[h_2(\boldsymbol{q}) - h_1(\boldsymbol{q})][h_2(\boldsymbol{q}') - h_1(\boldsymbol{q}')]\rangle. \quad (47)$$

Using Eqs. (35), (40), and (41) we have

$$\langle(\Delta\sigma_z)^2\rangle = \frac{2\,\pi\,E^2}{4\,(1-\nu^2)^2}\ q_L(\zeta q_L)^3\Delta\zeta\ \ [C_1(\zeta q_L) + C_2(\zeta q_L) - 2\eta\,\sqrt{C_1(\zeta q_L)C_2(\zeta q_L)}], \quad (48)$$

and

$$f(\zeta) = \frac{\pi\,E^2}{4\,(1-\nu^2)^2}\ q_L(\zeta q_L)^3\ [C_1(\zeta q_L) + C_2(\zeta q_L) - 2\eta\,\sqrt{C_1(\zeta q_L)C_2(\zeta q_L)}]. \quad (49)$$

The relative contact area, $P(\zeta)$, is obtained through Eqs. (8) and (9), where $f(\zeta)$ is obtained from Eq. (49). So $\gamma_{\text{eff}}(\zeta)$, the effective interfacial energy per area between an elastic solid and a hard substrate, both with randomly rough surfaces becomes [27-29]

$$\frac{\gamma_{\text{eff}}(\zeta)}{\Delta\gamma} = \frac{P(q_a)}{P(q_L)}\int_0^\infty dx\ (1+\xi^2x)^{1/2}\,e^{-x} - \frac{2\pi}{\delta}\,\alpha\int_{q_L}^{q_a} dq\ q^2[C_1(q) + C_2(q) - 2\eta\,\sqrt{C_1(q)C_2(q)}], \quad (50)$$

and for full contact, where $\alpha = 1$,

$$\frac{\gamma_{\text{eff}}(\zeta)}{\Delta\gamma} = \int_0^\infty dx\,(1+\xi^2 x)^{1/2}\,e^{-x} - \frac{2\pi}{\delta}\int_{q_L}^{q_a} dq\,q^2[C_1(q)+C_2(q) - 2\eta\sqrt{C_1(q)C_2(q)}]. \quad (51)$$

3.2 Contact area and interfacial surface separation for a non- adhesive contact

The new form of G and the relative contact area for elastic non-adhesive contact are obtained from Eqs. (17) and (24) through a substitution of the autocorrelation function $C(q)$ with the autocorrelation corresponding to $(h_2 - h_1)$, that is [27–29]

$$C(q) \to \left(C_1(q)+C_2(q)-2\eta\sqrt{C_1(q)C_2(q)}\right), \quad (52)$$

so, one could obtain:

$$G(q) = \frac{\pi}{4}\left(\frac{E}{1-\nu^2}\right)^2 \int_{q_L}^{q_a} dq\,q^3\left[C_1(q)+C_2(q) - 2\eta\sqrt{C_1(q)C_2(q)}\right]. \quad (53)$$

$$w(q) = \left(\pi\int_{q_L}^{q_a} dq\,q^3\left[C_1(q)+C_2(q) - 2\eta\sqrt{C_1(q)C_2(q)}\right]\right)^{-1/2}. \quad (54)$$

Using Eq. (24),

$$\frac{\partial P}{\partial\bar{u}} = \frac{2}{\sqrt{\pi}}\,S(q)\,exp\{-|S(q)|^2p^2\}\,\frac{dp}{d\bar{u}}. \quad (55)$$

Substituting Eqs. (42) and (55) in Eq. (22) results in

$$d\bar{u} = -\sqrt{\pi}\alpha\int_{q_L}^{q_a} dq\,q^2\left[C_1(q)+C_2(q) - 2\eta\sqrt{C_1(q)C_2(q)}\right] \times w(q)\exp\left\{-\left[\frac{w(q)p}{E^*}\right]^2\right\}\frac{dp}{p}. \quad (56)$$

Integrating this from $\bar{u} = 0$ (full contact, corresponding to p = ∞) to $\bar{u}$ gives

$$\bar{u} = \sqrt{\pi}\alpha\int_{q_L}^{q_a} dq\,q^2\left[C_1(q)+C_2(q) - 2\eta\sqrt{C_1(q)C_2(q)}\right] \times w(q)\int_p^\infty \frac{dp'}{p'}\,exp\left\{-\left[\frac{w(q)p'}{E^*}\right]^2\right\}. \quad (57)$$

For very low squeezing pressures, one has

$$p \approx \beta E^*\exp\left(-\frac{\bar{u}}{u_0}\right), \quad (58)$$

$$u_0 = \sqrt{\pi}\alpha\int_{q_L}^{q_a} dq\,q^2\left[C_1(q)+C_2(q) - 2\eta\sqrt{C_1(q)C_2(q)}\right]w(q), \quad (59)$$

$$\beta = \varepsilon\exp\left\{\int_{q_L}^{q_a}\left(C_1(q)+C_2(q) - 2\eta\sqrt{C_1(q)C_2(q)}\right)w(q)q^2\log\left(w(q)\right)dq \times\left(\int_{q_L}^{q_a}\left[C_1(q)+C_2(q) - 2\eta\sqrt{C_1(q)C_2(q)}\right]w(q)q^2dq\right)^{-1}\right\}, \quad (60)$$

with ε being obtained from Eq. (28).

3.3 Hysteretic contribution of rubber friction on the concrete surface when both surfaces are rough

Now consider that a randomly rough viscoelastic solid slide on a randomly rough hard substrate. Equation (29) holds, but here for full contact, the displacement of rubber is the difference between the fluctuations of the rubber and the substrate which is equivalent with Eq. (36), so with substituting the autocorrelation function C with the autocorrelation (Eq. (52)) the friction coefficient μ would be:

$$\mu = \frac{1}{2}\int_{q_0}^{q_a} dq\, q^3 \left[C_1(q) + C_2(q) - 2\eta\sqrt{C_1(q)C_2(q)}\right] P(q) \times \int_0^{2\pi} d\phi \cos\phi \,\mathrm{Im}\left[\frac{E(-qu\cos\phi)}{\sigma_0(1-\nu^2)}\right]. \quad (61)$$

As stated earlier, under the nominal stress σ_0, the surface asperities do not fully penetrate inside the rubber block and only a partial contact between the hard surface and the rubber block can be achieved. The introduction of the normalized contact area $P(q)$ in Eq. (61) takes this into account. Roughening the surface of the viscoelastic body changes the normalized contact area. The result for $G(q)$ would be (53) [27–29]

$$G(q) = \frac{1}{8}\int_{q_0}^{q_a} dq\, q^3 \left[C_1(q) + C_2(q) - 2\eta\sqrt{C_1(q)C_2(q)}\right] \int_0^{2\pi} d\phi \left|\frac{E(-qu\cos\phi)}{\sigma_0(1-\nu^2)}\right|^2. \quad (62)$$

In Eqs. (61) and (62), $C_1(q)$ and $C_2(q)$ are the auto spectral density functions of the rubber block and the concrete surface, respectively. The first, second, and third terms in Eqs. (61) and (62) show the relations between the coefficient of friction and thenormalized contact area with roughness of rubber block, roughness of substrate, and the roughness cross correlation between the rubber and the substrate, respectively. An explanation is in order here. It is assumed that parts of the rubber and the substrate which are in contact, both change with time. That is the case when a rubber wheel is rolling on the substrate, or when a rubber piece is rotating on a substrate around a rotation axis normal to the substrate. In such cases, the rubber and the substrate behave symmetrically. Otherwise, if a finite block of rubber is sliding on a larger substrate, with the contact part of the rubber being constant, the contact part of the substrate changes, and that of the rubber does not change. This is not the case studied here.

4 Numerical Results

In all cases considered below, the solids have self-affine fractal roughness. The auto-spectral density function for self-affine fractals can be described by [1,2,5,37,40]:

$$C(q) \approx \frac{H}{2\pi}\left(\frac{h_0}{q_0}\right)^2 \left(\frac{q}{q_0}\right)^{-2(H+1)}, \quad h_{rms} = \sqrt{\langle h^2\rangle} = \sqrt{\frac{(h_0)^2}{2}}. \quad (63)$$

H and h_{rms} are the Hurst exponent and the root-mean-square roughness of the solid, respectively. $q_0 = 2\pi/\xi$ is the roll-off wave number and ξ is the in-plane correlation length for the rough solid. $q_1 = 2\pi/a$ where a is the lattice constant (or the distance between the atoms).

4.1 Numerical Effective interfacial energy for an adhesive contact

The auto-spectral densities of the surfaces are obtained from Eq. (63). The following values are used

$$D_f = 2.2, \quad H = 0.8, \quad \Delta\gamma = \gamma_1 + \gamma_2 - \gamma_{12} = 100\frac{meV}{\dot{A}^2}, \quad \delta = 0.68\,\dot{A}. \quad (64)$$

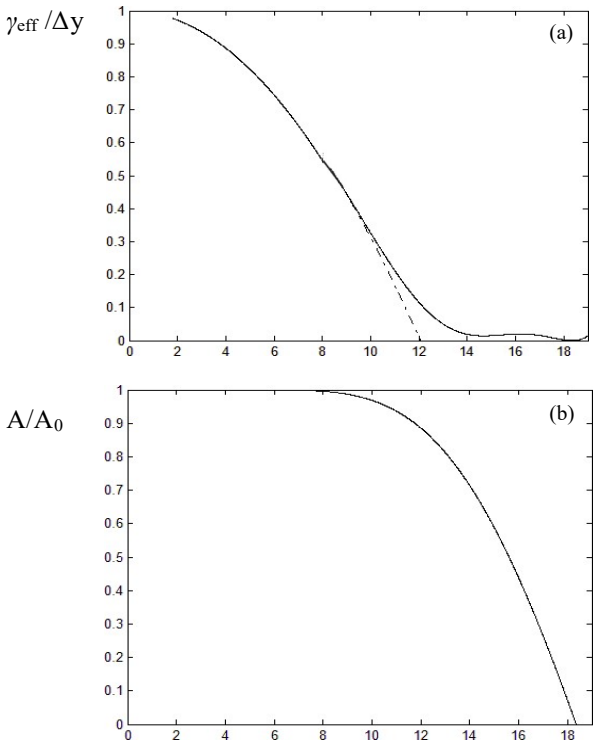

Figure 1. (a) The effective interfacial energy γ_{eff}, in units of the interfacial energy $\Delta\gamma$ for flat surfaces, as a function of the root-mean-square roughness of the substrate. The solid curve is the result of Persson's partial contact theory, and the dash-dot curve is the result of Persson's full contact theory. It is seen that for partial contact, the effective interfacial energy γ_{eff} vanishes in the root-mean-square roughness h_{rms} = 18.305 Å. (b) The area of real contact A, at the point where the external load vanishes, as a function of the root-mean- square roughness of the hard substrate, calculated using Persson's contact mechanics theory. The substrate surface is a self-affine fractal and the auto-spectral density functionis given by Eq. (63) with the Hurst exponent H = 0.8. One notes that A vanishes at the same root-mean-square roughness which makes γ_{eff} vanish.

If the only rough surface is the substrate, the result would be Fig. 1. If both surfaces are rough, there would be two independent self-affine rough surfaces characterized by (H_1, ξ_1, h_{1rms}) and (H_2, ξ_2, h_{2rms}). Taking the Hurst exponent of the two surfaces as $H_1 = H_2 = H = 0.8$, and their correlation lengths as $\xi_1 = \xi_2 = (2\pi/q_0)$, there remains the root-mean-square roughness of the two surfaces. The root-mean-square roughness of the elastic solid is taken to be 6 Å and that of the substrate is varied from 1 Å up to a value that the contact area vanishes.

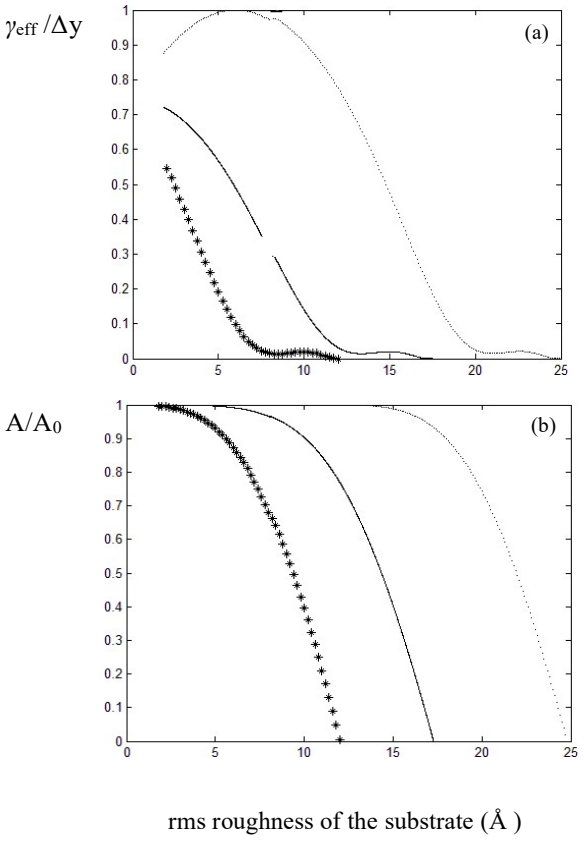

Figure 2. (a) The effective interfacial energy γ_{eff}, in units of the interfacial energy $\Delta\gamma$ for flat surfaces, as a function of the root-mean-square roughness of the substrate. The solidcurve is the result of Persson's partial contact theory. (b) The area of real contact A, at the point the external load vanishes, as a function of the root-mean- square roughness of the hard substrate, calculated using Persson's contact mechanics theory. The surfaces of the elastic solid and the hard substrate are self-affine fractals and the auto-spectral densities of the surfaces are obtained from Eq. (63) with Hurst exponents $H_1 = H_2 = H = 0.8$ and the correlation length $\xi_1' = \xi_2' = (2\pi/q_0)$. The surfaces are uncorrelated ($\eta = 0$) in the solid curve, completely positive correlated ($\eta = 1$) in the dotted curve, and completely negative correlated ($\eta = -1$) in the asterisk curve. The root-mean-square roughness of the elastic solid is 6 Å, and that of the substrate varies from 1 Å up to a value that the contact area vanishes.

Figure 2 shows the effective interfacial energy $\gamma_{eff}(\zeta)$ for partial contact and the contact area of real contact, as a function of the root-mean-square roughness of the hard substrate. In all these curves, both the surfaces are rough. However, the surfaces

are uncorrelated ($\eta = 0$) in the solid curve, completely positive correlated ($\eta = 1$) in the dotted curve, and completely negative correlated ($\eta = -1$) in the asterisk curve. It is seen that both surfaces are rough but uncorrelated which results in a decrease in the effective energy and the area of real contact compared to the case of only one rough surface. Introducing a positive correlation results in an increase in the effective energy. While the area of real contact, compared to the uncorrelated case; introducing a negative correlation result in a decrease in the effective energy and the area of real contact, compared to the uncorrelated case. This is seen, for example, through a comparison of the roughness at which the adhesion vanishes. The root-mean square roughness corresponding to this point is 18.305 Å when only one the substrate is rough, 17 Å when both surfaces are rough but uncorrelated, 24.742 Å when both surfaces are rough and the surfaces are completely positive correlated, and 12 Å when both surfaces are rough and the surfaces are completely negative correlated. Figure 2 also shows that for a positive correlation, increasing the root-mean-square roughness of the substrate from zero, makes the effective interfacial energy initially increase, and then decrease. This could be understood in the following way. The system with both surfaces rough, can be analyzed similar to a systemwith only one rough surface, if the following correlation C is used:

$$C(q) = C_1(q) + C_2(q) - 2\eta\sqrt{C_1(q)C_2(q)}. \quad (65)$$

It is seen that if η is positive, increasing C_1 from zero, makes the right-hand side of the above first decrease and then increase. For fixed C_2, the minimum value for C (corresponding with the maximum value for the effective interfacial energy) is obtained at

$$C_1 = \eta\, C_2, \quad (66)$$

If $\eta = 1$, then the minimum value is obtained when C_1 is the same as C_2. And it is seen in Fig. 2 that for $\eta = 1$ (the dotted curve) the maximum value for the effective interfacial energy is obtained when the root-mean-square roughness of the substrate is the same as that of the elastic solid.

4.2 Contact area and interfacial surface separation for a non-adhesive contact

For the auto-spectral densities of the surfaces of the hard substrate and the elastic block, the following values have been used:

$$q_L = 2 \times 10^8\, m^{-1}, \quad q_a = 4 \times 10^{10}\, m^{-1}, \quad (67)$$

$$H_1 = 0.8, \qquad h_{rms\,1} = 1\, nm\,,$$

$$H_2 = 0.8, \qquad h_{rms\,2} = 1\, nm\,, \quad (68)$$

$$E = 77.2\, GPa, \qquad \nu = 0.42. \quad (69)$$

Figure 3 shows the contact area ratio A/A_0 calculated from Eqs. (19) and (53), as a function of the normalized pressure p/E^* for the magnification $\zeta = 4$. The pressure distribution calculated from Eqs. (16) and (53), as a function of the normalized pressure σ/E^*, is shown in Fig. 4 for $\zeta = 4$ and for three different nominal pressures.

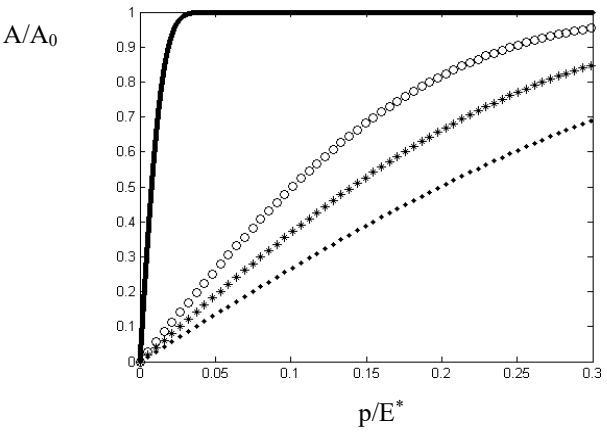

Figure 3: The contact area ratio A/A_0 as a function of the normalized pressure p/E^* for the magnification $\zeta = 4$. The circle curve is for the case where only the substrate is rough. The asterisk, solid, and dotted curves correspond to the case where both surfaces are rough and uncorrelated ($\eta = 0$), completely positively correlated ($\eta = 1$), and completely negatively correlated ($\eta = -1$), respectively.

In these curves, the circle curve is for the case where only the substrate is rough. The asterisk, solid, and dotted curves correspond to the case where both surfaces are rough and uncorrelated ($\eta = 0$), completely positively correlated ($\eta = 1$), and completely negatively correlated (η =-1), respectively. Figure 3 shows that both surfaces are rough, but uncorrelated, which results in a decrease in the contact area, compared to the case of only one rough surface. If both surfaces are rough, and they are correlated, depending on the sign of the correlation an increase or decrease in the values of the contact area is resulted, compared to the case of two uncorrelated surfaces and the case of only one rough surface. A positive correlation ($\eta = 1$) increases the contact area between the two surfaces, so that the pressure distribution vanishes in a smaller normalized pressure, as seen from Fig. 4. For a negative correlation η = -1, however, the contact area is decreased compared to the case of uncorrelated surfaces and the case of only rough surface, so that the pressure distribution vanishes in larger pressures. It is seen that when both surfaces are rough but uncorrelated, the width of the pressure distribution is larger compared to the case where only one surface is rough. A positive (negative) correlation results in a decrease (an increase) of the width of the pressure distribution.

The logarithm of the normalized average pressure p/E∗, as a function of the separation $\bar{u}$ between the average plane of the substrate and the average plane of the lower surface of the elastic block is shown in Fig. 5 corresponds to the magnification ζ = 4. In this curve, the circle curve is for the case where only the substrate is rough. The asterisk, solid, and dotted curves correspond to the case where both surfaces are rough and uncorrelated (η = 0), completely positively correlated (η = 1), and completely negatively correlated (η = -1), respectively. It is seen that the interfacial separation at a fixed pressure is larger when both surfaces are rough but uncorrelated. A positive (negative) correlation decreases (increases) the interfacial separation.

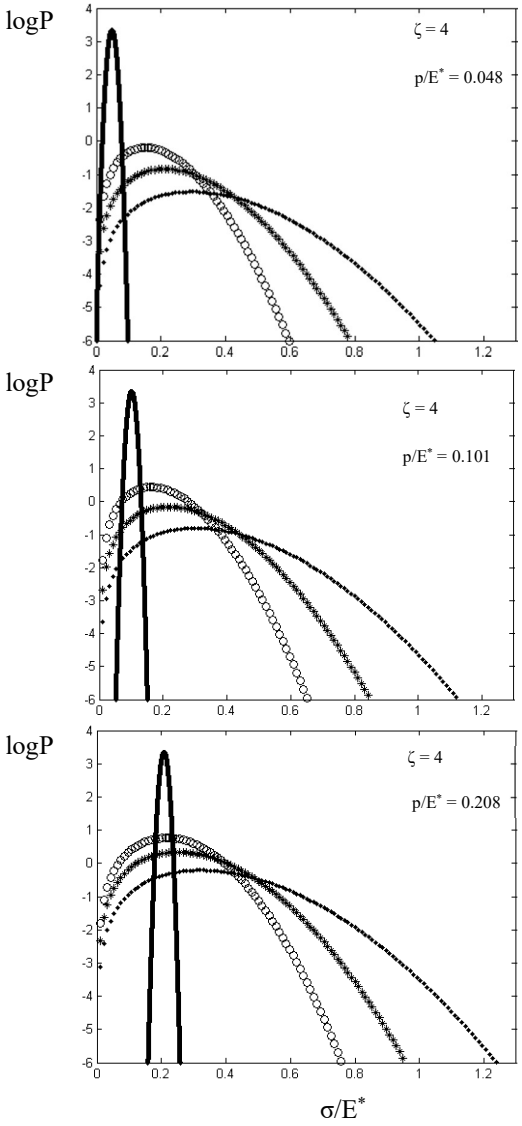

Figure 4. The pressure distribution as a function of the normalized pressure σ/E^* for the magnification $\zeta = 4$ and for three different nominal pressures. The circle curve is for the case where only the substrate is rough. The asterisk, solid, and dotted curves correspond to the case where both surfaces are rough and uncorrelated ($\eta = 0$), completely positively correlated ($\eta = 1$), and completely negatively correlated ($\eta = -1$), respectively.

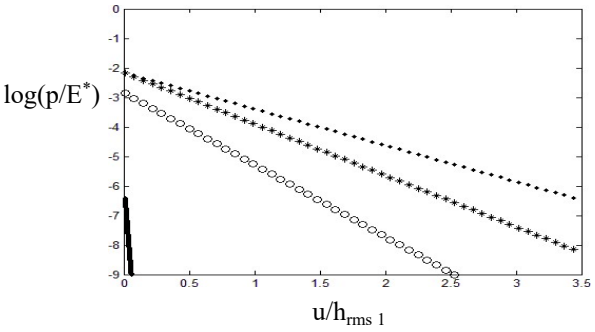

Figure 5. The logarithm of the normalized average pressure p/E^*, as a function of the separation $\overline{u}$ between the average plane of the substrate and the average plane of the lower surface of the elastic block for the magnification $\zeta = 4$. The circle curve is for the case where only the substrate is rough. The asterisk, solid, and dotted curves correspond to the case where both surfaces are rough and uncorrelated ($\eta = 0$), completely positively correlated ($\eta = 1$), and completely negatively correlated ($\eta = -1$), respectively.

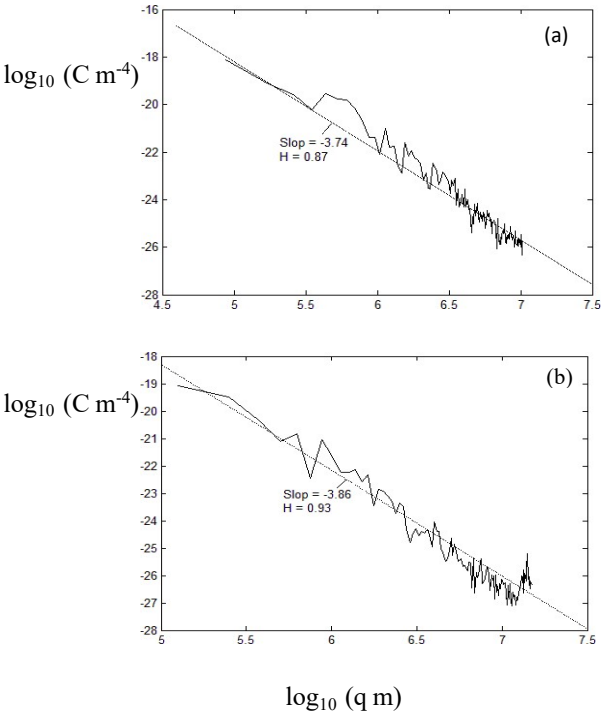

Figure 6. (a) The auto spectral density function, as a function of the wave number q for the polished rubber block. The dashed line has the slope $-2(1+H_1) = -3.74$ corresponding to the Hurst exponents $H_1 = 0.87$ and fractal dimension $D_f = 3-H_1 = 2.13$. The root-mean- square roughness is 6 μm. (b) The auto spectral density function, as a function of the wave number q for the concrete surface. The dashed line has the slope $-2(1+H_2) = -3.86$ corresponding to the Hurst exponents $H_2 = 0.93$ and fractal dimension $D_f = 3 - H_2 = 2.07$. The root-mean-square roughness is 2.7 μm.

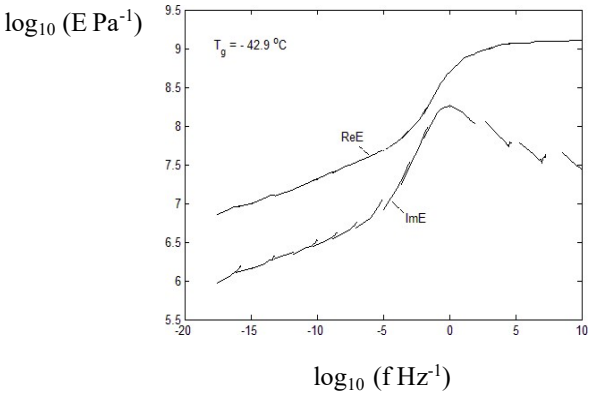

Figure 7. The real (upper curve) and the imaginary part (lower curve) of the viscoelastic modulus as a function of frequency at the glass transition temperature Tg = 42.9°C for the rubber tread compound.

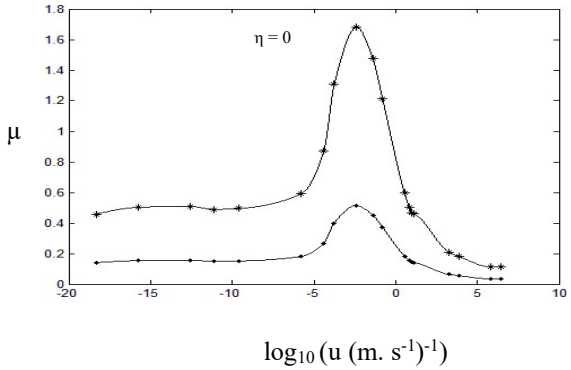

Figure 8. The friction coefficient versus the sliding velocity for the tire tread compound, with no flash temperature effect [24]. The upper curve with asterisk markers corresponds to both surfaces being rough but uncorrelated, the lower curve with point markers to only the substrate being rough. The reference temperature is $T = 25$°C.

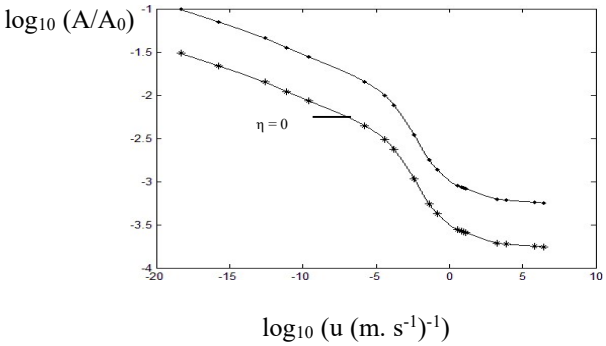

Figure 9. The relative real-contact area versus the sliding velocity. The lower curve with asterisk markers corresponds to both surfaces being rough but uncorrelated, the upper curve with point markers corresponds to when only the substrate is rough. The reference temperature is $T = 25$°C.

4.3 Hysteretic contribution of rubber friction on the concrete surface when both surfaces are rough

In all cases considered below, the viscoelastic solid is a polished rubber block where the substrate is a concrete surface with auto-spectral density functions (Fig. 6). Also, we have used the viscoelastic modulus of the rubber block in Fig. 7 with the reference temperature T=25°C. The nominal squeezing pressure is σ_0 = 0.4 MPa.

Figure 8 is the friction coefficient versus the sliding velocity for the polished tire tread compound, with no flash temperature effect [24]. The upper curve with asterisk markers corresponds to both surfaces being rough but uncorrelated, the lower curve with point markers corresponds to when only the substrate is rough. The reference temperature is T = 25°C.

Figure 9 is the relative real-contact area versus the sliding velocity. The lower curve with asterisk markers corresponds to both surfaces being rough but uncorrelated, the lower curve with point markers corresponds to when only the substrate is rough. It is seen that the real contact area is less, hence the friction is more, when both surfaces are rough. If both the rubber and the substrate are rough and correlated, depending on the sign of correlation an increase or decrease in the values of the friction is resulted compared to the case of two uncorrelated surfaces. The rough viscoelastic solid and the rough substrate are assumed to be correlated with parameters similar to the previous section. Figure 10 shows that $\eta = 1$ (a positive correlation) decreases the friction between the two surfaces and η = -1 (a negative correlation) increases the friction between the two surfaces compared to uncorrelated surfaces, with the same roughness parameters. The real-contact area for $\eta = 1$ and $\eta = -1$ are shown in Fig. 11.

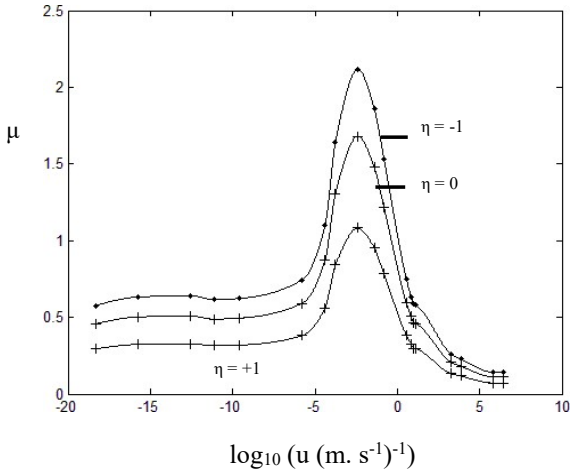

Figure 10. The friction coefficient versus the sliding velocity for the tire tread compound, without the flash temperature effect. No correlation: the middle curve with asterisk markers. Complete positive correlation: the lower curve with plus sign markers. Complete negative correlation: the upper curve with point markers. The reference temperature is T = 25°C.

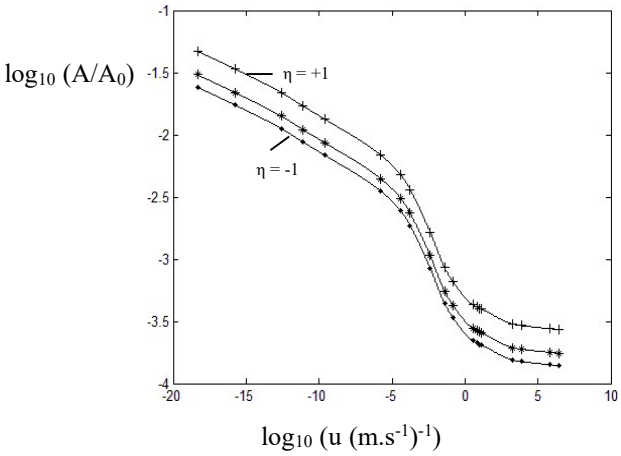

Figure 11. The relative area of real contact versus the sliding velocity, without the flash temperature effect. No correlation: the middle curve with asterisk markers. Complete positive correlation: the upper curve with plus sign markers. Complete negative correlation: the lower curve with point markers. The reference temperature is T = 25°C.

4 Concluding remarks

We reviewed Persson's contact mechanics theory. We also reviewed the extended version of Persson's contact mechanics theory. In the extended version, we

presented that a case where both surfaces are rough can be mapped into a case of only one surface being rough, this is possible only if one removes the constraint that the rough surfaces of the latter be self-similar. So, there is no general mapping between systems of both surfaces being rough and self-similar, and those with only one surface being rough and self-similar.

The extended version depicted that in the case where both surfaces are rough, it could happen that increasing the roughness of one surface increases the effective interfacial energy. This is in contrast with the case of only one surface being rough, where increasing the roughness always results in a decrease in the effective interfacial energy. The results were seen to be depending on the correlation between the roughness of the two surfaces. Specifically, it was shown that when the two surfaces are uncorrelated, the real contact area and the adhesion is less compared to the case where only the substrate is rough.

It was also shown that when the surfaces are correlated, a positive correlation increases the real contact area and the adhesion compared to the case of no correlation. This is while a negative correlation decreases the real contact area and the adhesion compared to the case of no correlation. A reverse pattern is seen for the width of the pressure distribution, the interfacial separation (at equal pressures), as well as the friction; However, these parameters experience an increase when both surfaces are rough but uncorrelated, while they experience a decrease (an increase) when a positive (negative) correlation exists.

Acknowledgements

This work was financially supported by Alzahra University.

References

[1] B. N. J. Persson, "Theory of rubber friction and contact mechanics." Journal of Chemical Physics, **115** (2001) 3840.

[2] B. N. J. Persson, "Adhesion between an elastic body and a randomly rough hard surface." The European Physical Journal E, 8 (2002) 385.

[3] F. P. Bowden, and D. Tabor, Friction and Lubrication of Solids, Wiley, New York, 1956.

[4] K. L. Johnson, Contact Mechanics, Cambridge University Press, Cambridge, 1966.

[5] B. N. J. Persson, Sliding Friction: Physical Principles and Applications, 2nd ed., Springer, Heidelberg, 2000.

[6] A. I. Volokitin, and B. N. J. Persson, "Near-field radiative heat transfer and noncontact friction." Reviews of Modern Physics, **79** (2007) 1291.

[7] E. Rabinowicz, Friction and Wear of Materials, 2nd ed., Wiley, New York, 1995.

[8] N. Patir, and H. S. Cheng, "Application of Average Flow Model to Lubrication Between Rough Sliding Surfaces." Journal of Lubrication Technology. **101** (1979) 220.

[9] H. Hertz, "On the contact of elastic solids." Journal fur die Reine Angewandte Mathematk, **92** (1881) 156-171.

[10] J. Greenwood, and J. Williamson, "Contact of nominally flat surfaces." Proceedings of the Royal Society of London. Series A, **295** (1966) 300.

[11] B. N. J. Persson, "Elastoplastic contact between randomly rough surfaces." Physical Review Letters, **87** (2001) 116101.

[12] B. N. J. Persson, "Contact mechanics for randomly rough surfaces." Surface Science Reports, **61** (2006) 201.

[13] B. N. J. Persson, F. Bucher, and B. Chiaia, "Elastic contact between randomly rough surfaces: Comparison of theory with numerical results." Physical Review B, **65**

(2002) 184106.

[14] B. N. J. Persson, "Adhesion between Elastic Bodies with Randomly Rough Surfaces." Physical Review Letters, **89** (2002) 245502.

[15] N. Mulakaluri, and B. N. J. Persson, "Adhesion between elastic solids with randomly rough surfaces: Comparison of analytical theory with molecular-dynamics simulations." Europhysics Letters, **96** (2011) 66003.

[16] B. N. J. Persson, "On the elastic energy and stress correlation in the contact between elastic solids with randomly rough surfaces." Journal of Physics: Condensed Matter, **20** (2008) 312001.

[17] B. N. J. Persson, and E. Tosatti, "The effect of surface roughness on the adhesion of elastic solids." Journal of Chemical Physics, **115** (2001) 5597.

[18] C. Yang, U. Tartaglino, and B. N. J. Persson, "Influence of surface roughness on superhydrophobicity." Physical Review Letters, **97** (2006) 116103.

[19] B. N. J. Persson, "On the theory of rubber friction." Surface Science, 401 (1998) 445.

[20] B. N. J. Persson, and M. Scaraggi, " Theory of adhesion: Role of surface roughness." The Journal of Chemical Physics, **141** (2014) 124701.

[21] B. N. J. Persson, "Rubber friction on wet and dry road surfaces: The sealing effect ." Physical Review B, **71** (2005) 035428.

[22] B. Lorenz, B. N. J. Persson, G. Fortunato, M. Giustiniano, and F. Baldoni, "Rubber friction for tire tread compound on road surfaces." Journal of Physics: Condensed Matter, **25** (2013) 1.

[23] B. Lorenz, B. N. J. Persson, S. Dieluweit, and T. Tada, "Rubber friction: Comparison of theory with experiment." European Physical Journal E, 34 (2011) 129.

[24] B. N. J. Persson, "Rubber friction: role of the flash temperature." Journal of Physics: Condensed Matter, **18** (2006) 7789.

[25] A. A. Griffith, "The Phenomena of Rupture and Flow in Solids." Philosophical Transactions: Royal Society, London, Series A, **222** (1920) 163.

[26] B. N. J. Persson, U. Tartaglino, E. Tosatti, and H. Ueba, "Electronic friction and liquid-flow-induced voltage in nanotubes." Physical Review B, **69** (2004) 235410.

[27] M. Feshanjerdi, A. A. Masoudi, and M. Khorrami, "Surface coupling effects on the adhesive contact between an elastic solid and a hard substrate with randomly rough, self-affine fractal surfaces." Journal of Statistical Mechanics: Theory and Experiment, **2015** (2015) P02018.

[28] M. Feshanjerdi, M. Khorrami, and A. A. Masoudi, "The hysteretic contribution of friction for the polished rubber on the concrete surface." Applied Surface Science **394** (2017) 528.

[29] M. Feshanjerdi, A. A. Masoudi, and M. Khorrami, "Surface coupling effects on contact mechanics: contact area and interfacial separation between an elastic solid and a hard substrate with randomly rough, self-affine fractal surfaces." Journal of Theoretical and Applied Physics, **11** (2017) 71.

[30] C. Yang, and B. N. J. Persson, "Contact mechanics: contact area and interfacial separation from small contact to full contact." Journal of Physics: Condensed Matter, **20** (2008) 215214.

[31] B. N. J. Persson, O. Albohr, U. Tartaglino, A. I.

Volokitin, and E. Tosatti, " On the nature of surface roughness with application to contact mechanics, sealing, rubber friction and adhesion." Journal of Physics: Condensed Matter, **17** (2005) R1.

[32] B. N. J. Persson, "Relation between interfacial separation and load: a general theory of contact mechanics." Physical Review Letters, **99** (2007) 125502.

[33] L. Mandel, and E. Wolf, Optical Coherence and Quantum Optics, Cambridge university press, Cambridge, 1995.

[34] J. S. Bendat, and A. G. Piersol, Engineering Applications of Correlation and Spectral Analysis, 2nd edn., Wiley, New York, 2013.

[35] Y. Zhao, G. C. Wang, and T. M. Lu, Characterization of Amorghous and Crystalline Rough Surface: Principles and Applications, Academic press, Waltham 2000.

[36] J. S. Bendat, and A. G. Piersol, Random Data: Analysis and Measurement Proce-dures, 3rd edn., Wiley, New York, 2000.

[37] G. Palasantzas, J. Barnas, and J. T. M. De. Hosson, "Correlated roughness effects on electrical conductivity of quantum wires." Journal of Applied Physics, **89** (2001) 8002.

[38] G. Carbone, B. Lorenz, B. N. J. Persson, and A. Wohlers, "Contact mechanics and rubber friction for randomly rough surfaces with anisotropic statistical properties." The European Physical Journal E, **29** (2009) 275.

[39] V. Jankauskaitė, K. Žukienė, and S. Petraitienė, "Quantitative description of polychloroprene and piperylene–styrene blend films surface morphology." Polymer Engineering & Science, **47** (2007) 824.